

Article

Impact of COVID-19 Lockdown on Inhaled Toxic Elements in PM_{2.5} in Beijing: Composition Characterization and Source-Specific Health Risks Assessment

Mingsheng Zhao, Lihong Ren ^{*}, Xiaoyang Yang, Yuanguan Gao, Gang Li and Yani Liu

State Key Laboratory of Environmental Criteria and Risk Assessment, Chinese Research Academy of Environmental Sciences, Beijing 100012, China; ligang01@craes.org.cn (G.L.)

* Correspondence: renlh@craes.org.cn

Abstract: In early 2020, China experienced a mass outbreak of a novel coronavirus disease (COVID-19). With an aim to evaluate the impact of emission variations on toxic element species in PM_{2.5} and the health risks associated with inhalation exposure during COVID-19, we collected PM_{2.5} filter samples in Beijing from January 1 to February 28, 2020. Positive matrix factorization (PMF) and a health risk (HR) assessment model were used to assess the health risks of the toxic elements and critical risk sources. The total concentration of eight toxic elements (Se, Cd, Pb, Zn, As, Cu, Ni, and Cr) in Beijing showed a trend of first increasing and then decreasing: full lockdown (322.9 ng m⁻³) > pre-lockdown (264.2 ng m⁻³) > partial lockdown (245.3 ng m⁻³). During the lockdown period, stringent control measures resulted in significant reductions (6–20%) in Zn, Pb, Cd, and Ni levels, while concentrations of Se, As, Cu, and Cr were unexpectedly elevated (14–348%). A total of five sources was identified: traffic emission, coal combustion, dust emission, industrial emission and mixed source of biomass burning and firework combustion. Total carcinogenic risk (TCR) of the selected toxic elements exceeded the US EPA limits for children and adults. As and Cr (IV) were the main contributors to non-carcinogenic and carcinogenic risks, respectively. For source-resolved risks, coal combustion was the main contributor to HI (43%), while industrial emissions were the main cause of TCR (45%). Additionally, increased contributions from coal combustion, biomass burning, and firework combustion during the full lockdown elevated the HI and TCR values.

Keywords: COVID-19; Beijing; toxic elements; health risk assessments; source apportionment



Citation: Zhao, M.; Ren, L.; Yang, X.; Gao, Y.; Li, G.; Liu, Y. Impact of COVID-19 Lockdown on Inhaled Toxic Elements in PM_{2.5} in Beijing: Composition Characterization and Source-Specific Health Risks Assessment. *Atmosphere* **2024**, *15*, 563. <https://doi.org/10.3390/atmos15050563>

Academic Editors: Daniele Contini and Haider A. Khwaja

Received: 22 February 2024

Revised: 3 April 2024

Accepted: 25 April 2024

Published: 30 April 2024



Copyright: © 2024 by the authors. Licensee MDPI, Basel, Switzerland. This article is an open access article distributed under the terms and conditions of the Creative Commons Attribution (CC BY) license (<https://creativecommons.org/licenses/by/4.0/>).

1. Introduction

Toxic elements are a key component of PM_{2.5} and play an essential part in health risks because of their bioavailability and accumulation [1–4]. The toxic elements in PM_{2.5} may raise the risk of cardiopulmonary-related diseases and are therefore a matter of great concern [5–7]. The sources of toxic elements are more complex, and they can originate from the combustion of fossil fuels, vehicles, industries, building sites, resuspended dust, and long-distance transportation [6,8,9]. Changes in emission sources can affect the concentration of toxic elements, consequently leading to alterations in health risks. Therefore, studying the health risks associated with toxic elements and understanding the impact of changes in emission sources on human health risks is essential to further optimize human health protection.

The public's attention has been widely drawn to the human health risks associated with toxic elements in recent years [10–13]. Yang et al. [14] revealed the non-carcinogenic and carcinogenic risks associated with breathing-in exposure to toxic elements in PM_{2.5} in the Beijing area, with the non-carcinogenic risk being primarily caused by As, while the carcinogenic risk getting mainly attributed to Cr. Li et al. [15] summed up the health risks of Cd, Cr, As, Pb, Cu, Zn, and Ni in 27 major cities in China from 2013 to 2019 and found that As and Cr were the primary factors contributing to non-carcinogenic and carcinogenic

risk, respectively. Recent investigations into element pollution have concentrated on the health risks of individual elements [16–18].

PM_{2.5}-bound elements have different toxicities, and their sources are more complex [19,20]. Assessing the health risks of different pollution sources can aid in the identification of health risks and abatement potential of exposure to different sources of PM_{2.5} [21,22]. Certain studies have integrated source apportionment of PM_{2.5}; however, source contributions to toxic elements varied greatly from source contributions to the health risks to locals [7,10,23]. Hence, from the perspective of protecting human health, source apportionment should be combined with health risk assessment to estimate source-specific health risks in order to prioritize control of emissions, rather than only estimating the contribution of specific sources to ambient concentrations. However, only a few case studies have combined health risks and source apportionment to quantify source-specific health risks for toxic elements [24–26]. The research has focused only on individual toxic elements, and combining health risks and source apportionment has mainly been overlooked, while the impact of emission control measures on toxic elements and their health risk is poorly understood.

In early 2020, a large-scale outbreak of a novel coronavirus disease (COVID-19) occurred in China [27]. The Chinese government imposed stringent nationwide lockdown measures, such as quarantines, transport stoppages, and commercial closures, in an effort to stop the outbreak's spread [28]. This led to a dramatic drop in pollutants across the country [29]. The strict quarantine measures taken to control COVID-19 have benefited the quality of air across China within the short term, with significant reductions in concentrations of PM_{2.5}, CO, and NO₂ [22]. However, little research has been performed on the effects of emission changes on toxic elemental species in PM_{2.5} during the COVID-19 lockdown [30] and whether the health risks of toxic elements in the environment decreased during the lockdown period, and whether the source-specific health risks have changed are unclear.

Therefore, in this study, human health risks assessment and pollution source apportionment contributions were combined with an aim to focus on assessing the health risks in Beijing during different lockdown periods owing to COVID-19. Another objective of this study was to identify key toxic elements and major pollution sources that require regulation from the point of view of efficiently decreasing health risks and pollution source contributions. The results of this study will help to develop effective strategies to reduce the release of toxic elements and minimize public health risks.

2. Materials and Methods

2.1. Study Sites

Beijing is a typical representative city of the Beijing–Tianjin–Hebei region and a megacity in northern China, where air quality is of great concern. Compared to other cities in China, Beijing is a more ideal location for the study of atmospheric pollution in the northern region. Following the COVID-19 outbreak, the Chinese government activated the strictest level of closure measures on 24 January 2020. These measures have led to significant changes in emission levels, thereby providing a chance to survey key controlling sources that are effective in reducing the health risks associated with environmental toxic elements. The research site in Beijing is located at the Chinese Research Academy of Environmental Sciences (40.04° N, 116.41° E), near the fifth ring road. The sampling site is located on the roof of the building at a distance of about 10 m from the ground. Additional details about the area surrounding the sampling site are presented in Table S1.

The sampling of PM_{2.5} was performed in Beijing from 1 January 2020 to 28 February 2020. Based on government interventions and the resumption of activities by several industries and firms in Beijing [22,31], three periods were selected to explain the changes in the emissions from the different sources. These periods are pre-lockdown (1–23 January 2020), full lockdown (24 January to 9 February 2020), and partial lockdown (10–29 February 2020).

2.2. Sampling and Chemical Analyses

Throughout the study period, ambient PM_{2.5} samples were collected with a four-channel low-volume air sampler (H-16A, TH. Ltd., Wuhan, China). One sampling channel was fitted with a Teflon filter (PTFE, Pall Corporation, New York, NY, USA), and the other with a quartz filter (Quartz Microfiber Filter, Pall Corporation, New York, NY, USA) for PM_{2.5} collection. The sample collection period was 23 h, from 10:00 to 09:00 the following day. Blank field samples were collected simultaneously at the sampling point for quality assurance and control (QA/QC).

Half of the Teflon filter was digested with acid prior to instrumental analysis using an inductively coupled plasma mass spectrometer (ICP-MS, Agilent Technologies, Inc., Santa Clara, CA, USA) for 17 trace elements (Na, Mg, Al, K, Ca, Fe, V, Cr, Mn, Ni, Cu, Zn, As, Se, Cd, Ba, and Pb). Eight carbon fractions (OC1, OC2, OC3, OC4, EC1, EC2, EC3, and OP) were analyzed in each quartz fiber filter (0.5 cm²) using a thermo-optical carbon analyzer (DRI-2001A, Atmospheric Inc., Tucson, AZ, USA) and following the IMPROVE_A protocol. For more information on the analytical procedures and QA/QC, please refer to Text S1 in the Supplementary Material.

2.3. Analysis Methods

2.3.1. Health Risk (HR) Model

Studies have found that excessive exposure to heavy metals combined with PM_{2.5} can threaten human health, causing respiratory irritation and inflammation, lung disease, cardiovascular disease, and heart disease, and some toxic elements can also lead to an increased risk of cancer [6,10]. Based on relevant studies by the Integrated Risk Information System (IRIS) and International Agency for Research on Cancer (IARC), contaminants are classified as non-carcinogens and carcinogens [6,32]. Se, Cd, Pb, Zn, As, Cu, Ni, and Cr (VI) are non-carcinogens, whereas Cd, Pb, As, Cr (VI), and Ni are carcinogens or possible carcinogens [32]. For the purpose of assessing health risks, the concentration of Cr (VI) is 1/7 of the total Cr concentration [22]. Inhalation is the main pathway for exposure to PM_{2.5}; therefore, we assessed the risks to the health of both children and adults from inhalation exposure to toxic elements [24,26].

The exposure concentration by inhalation route was calculated as below:

$$EC_j = C_j \times \frac{ET \times EF \times ED}{AT_n} \quad (1)$$

where EC_j and C_j denote the exposure concentration ($\mu\text{g}\cdot\text{m}^{-3}$) of the j th non-carcinogen and carcinogen by inhalation and the j th toxic element ($\mu\text{g}\cdot\text{m}^{-3}$) in PM_{2.5}, respectively; ET , ED , EF , and AT_n denote exposure time ($\text{h}\cdot\text{d}^{-1}$), exposure duration (y), exposure frequency ($\text{d}\cdot\text{y}^{-1}$), and average lifetime (h), respectively. Table S2 presents the ET , EF , ED , and AT_n values for the different groups [8].

The non-carcinogenic and carcinogenic risks in this study were calculated according to the following equations [33]:

$$HQ_j = \frac{EC_j}{RfC_j \times 1000} \quad (2)$$

$$HI = \sum HQ_j \quad (3)$$

$$CR_j = EC_j \times IUR \quad (4)$$

$$TCR = \sum CR_j \quad (5)$$

where HQ_j and HI are the non-carcinogenic risk for element j and the total non-carcinogenic risk for the selected toxic elements, respectively (unitless); CR_j and TCR are the carcinogenic risk for element j and the total carcinogenic risk for the selected toxic elements, respectively (unitless); RfC_j and IUR are the inhalation reference concentration ($\text{mg}\cdot\text{m}^{-3}$) and the

inhalation unit risk ($(\mu\text{g}\cdot\text{m}^{-3})^{-1}$), respectively. The RfC_j and IUR values are presented in Table S3.

Based on US EPA [34] metrics for non-carcinogenic risk, $HQ (HI) \leq 1$ is considered acceptable and $HQ (HI) > 1$ is considered not acceptable; $CR (TCR) \leq 10^{-6}$ is acceptable and $CR (TCR) > 10^{-6}$ is unacceptable [16]. Higher $HQ (HI)$ and $CR (TCR)$ values indicate higher non-carcinogenic and carcinogenic risks [22].

2.3.2. PMF Model

A positive matrix factorization (PMF) receptor model was used to identify and quantify the main sources of these elements [10,35]. The principle is to decompose the sample set (X) into source profile (F) and source contribution (G) [36], examine the distribution of each species using feature Q (robust), and assess the feasibility of the solution. The receptor model requires two inputs to run PMF, namely concentration and its uncertainty. Below the minimum detection limit (MDL), the data were substituted with half of the MDL, and the uncertainty was established at 5/6th of the MDL. The corresponding instability of the data above the MDL was computed using Equation (6) [6,14]. Different source numbers were tested by applying a trial to determine the optimal solutions. The identification of sources was conducted based on major marker species [10].

$$Uncertainty = \sqrt{(Error\ Fraction \cdot concentration)^2 + (0.5 \cdot MDL)^2} \quad (6)$$

Table S4 presents the MDLs of the resolved species. For more details on PMF analyses and data processing, refer to the Supplementary Materials.

2.3.3. PMF–HR Model

In this section, we combined health risk and source apportionment to assess the health risks of different emission sources [26].

Step 1: Calculate the concentrations of toxic elements from different sources:

$$C_{ij}^k = g_i^k \cdot f_j^k \quad (7)$$

where C_{ij}^k , g_i^k , and f_j^k are the concentration of element j in the i th sample from the k th source ($\mu\text{g}\cdot\text{m}^{-3}$), the concentration of the k th source contributing to the i th sample ($\mu\text{g}\cdot\text{m}^{-3}$), and the quality fraction of element j in the k th source, respectively;

Step 2: The exposure dose of toxic elements from different sources is calculated as follows:

$$EC_{ij}^k = C_{ij}^k \times \frac{ET \times EF \times ED}{AT_n} \quad (8)$$

where EC_{ij}^k denotes the exposure concentration ($\mu\text{g}\cdot\text{m}^{-3}$) of the j th non-carcinogen and carcinogen by inhalation; C_{ij}^k has the same definition and value as in Equation (7). For ET , EF , ED , and AT_n , the definitions and values are identical to those in Equation (1);

Step 3: Perform health risk assessments related to each pollution source:

$$HQ_{ij}^k = \frac{EC_{ij}^k}{RfC_j \times 1000} \quad (9)$$

$$HI_i^k = \sum HQ_{ij}^k \quad (10)$$

$$CR_{ij}^k = EC_{ij}^k \times IUR \quad (11)$$

$$TCR_i^k = \sum CR_{ij}^k \quad (12)$$

where HQ_{ij}^k and HI_i^k are the hazard quotient of the j th element of the k th source and the hazard index of the k th source in the i th sample, respectively. CR_{ij}^k and TCR_i^k are the cancer risks for the j th element from the k th source in the i th sample and the total cancer risk from

the k th source, respectively. RfC_j and IUR are defined as and have the same values as those in Equations (2) and (4).

3. Results and Discussion

3.1. Composition Characterization

3.1.1. Characterization of PM_{2.5} Concentration

The average concentration ($\mu\text{g}\cdot\text{m}^{-3}$) of PM_{2.5} in Beijing during different periods is shown in Figure 1. Throughout the study period, the average concentration of PM_{2.5} in Beijing was slightly higher than China's 24 h ambient air quality standard ($75 \mu\text{g}\cdot\text{m}^{-3}$) and 3.0 times higher than the daily standard value recommended by the World Health Organization (WHO) ($25 \mu\text{g}\cdot\text{m}^{-3}$) [8]. The results showed that Beijing experienced more severe PM_{2.5} pollution during the study period. In addition, the PM_{2.5} concentration in Beijing during different periods was in the order of full lockdown ($89.9 \mu\text{g}\cdot\text{m}^{-3}$) > partial lockdown ($75.7 \mu\text{g}\cdot\text{m}^{-3}$) > pre-lockdown ($64.6 \mu\text{g}\cdot\text{m}^{-3}$). The PM_{2.5} concentration is primarily influenced by emissions from pollution sources, secondary transformation, and regional transport [37]. Despite the significant reduction in major emission pollutants during the COVID-19 shutdown period, the imbalanced emission reductions in NO_x and VOC resulted in an unexpected increase in levels of PM_{2.5} in Beijing [38]. In addition, unfavorable weather conditions have the potential to exacerbate PM_{2.5} pollution. During the full lockdown in Beijing, relative humidity increased from 46.6% to 55.7%, while wind speed reduced from $2.4 \text{ m}\cdot\text{s}^{-1}$ to $1.9 \text{ m}\cdot\text{s}^{-1}$ compared to the pre-lockdown period (Figure S2). Therefore, the PM_{2.5} exhibited the highest concentration during the full lockdown.

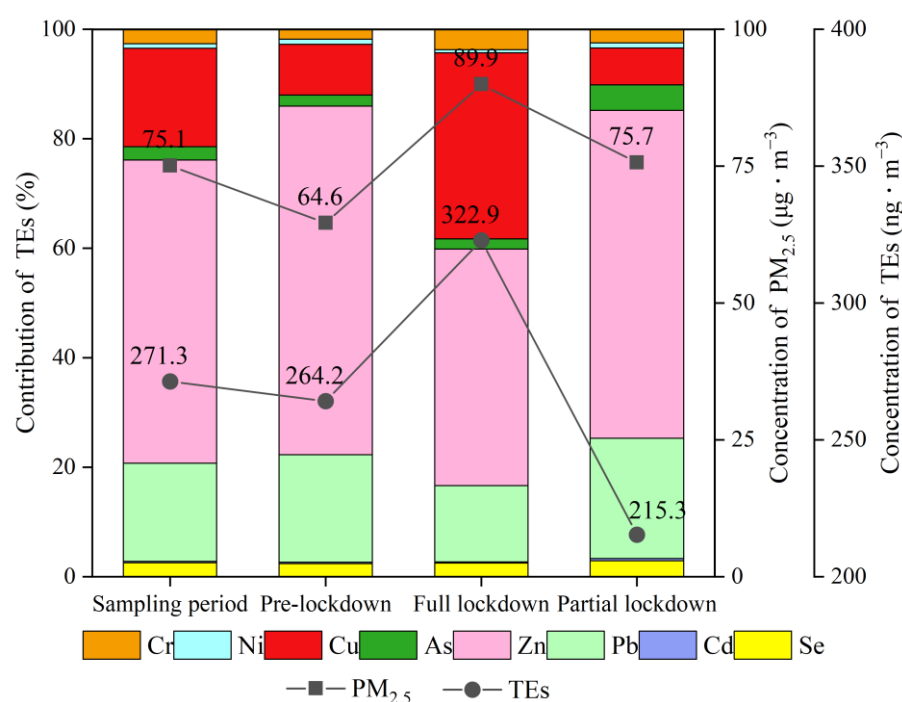


Figure 1. The PM_{2.5} concentrations ($\mu\text{g}\cdot\text{m}^{-3}$), total concentrations ($\text{ng}\cdot\text{m}^{-3}$) of selected TEs, and the relative contribution of each toxic element to the total element concentration (%).

3.1.2. Concentrations of PM_{2.5}-Bound Elements

The PM_{2.5}-bound toxic elements (TEs), including Se, Cd, Pb, Zn, As, Cu, Ni, and Cr, were used for analysis in this study. The concentrations ($\mu\text{g}\cdot\text{m}^{-3}$) and percentages (%) of selected TEs in Beijing at different periods are presented in Table 1 and Figure 2. The mean concentration of the eight selected toxic elements and their contribution to PM_{2.5} were $271.3 \text{ ng}\cdot\text{m}^{-3}$ and 0.36%, respectively, while the average concentration of Zn ($150.2 \text{ ng}\cdot\text{m}^{-3}$) were higher than those of the other toxic elements, followed by that of Cu ($48.8 \text{ ng}\cdot\text{m}^{-3}$) and Pb ($48.7 \text{ ng}\cdot\text{m}^{-3}$), while that of Ni ($2.2 \text{ ng}\cdot\text{m}^{-3}$) and Cd ($0.7 \text{ ng}\cdot\text{m}^{-3}$) were the lowest.

Zn was also reported by Wang et al. [22] and Diao et al. [26] to be the most highly abundant toxic element for PM_{2.5} in northern Chinese cities. Therefore, Zn-related emission sources (e.g., coal combustion, traffic, and industrial emissions) should be emphasized.

Table 1. The concentrations (ng·m⁻³) of the selected toxic elements in Beijing during the whole sampling period and different COVID-19 lockdown periods.

Species	Sampling Period		Pre-Lockdown		Full Lockdown		Partial Lockdown	
	Mean	StDev	Mean	StDev	Mean	StDev	Mean	StDev
Se	6.9	4.3	6.3	3.2	8.2	5.6	6.3	3.5
Cd	0.7	0.4	0.7	0.4	0.7	0.4	0.9	0.4
Pb	48.7	26.8	51.9	30.3	44.9	25.2	47.2	19.5
Zn	150.2	91.9	168.2	113.8	139.5	69.1	129.0	56.6
As	6.6	4.2	5.3	2.6	6.0	3.9	10.0	5.2
Cu	53.8	118.0	24.5	32.7	125.7	187.1	14.5	25.2
Ni	2.2	2.0	2.4	2.4	1.9	1.4	2.0	1.8
Cr	7.2	8.5	4.9	3.3	12.0	13.2	5.4	3.6
Total	271.3	185.6	264.2	163.1	322.9	243.0	215.3	98.2

To better understand the levels of toxic elements in the ambient air in Beijing, the concentration levels of selected toxic elements were evaluated based on the current National Ambient Air Quality Standards (NAAQS) of China (GB 3095-2012) and WHO standards [37]. Compared with the limit values of the NAAQS of China (GB 3095-2012) (6 ng·m⁻³ for As and 0.025 ng·m⁻³ for Cr), the mean concentrations of As (6.6 ng·m⁻³) and Cr (7.2 ng·m⁻³) were significantly higher during the study period. The concentrations of Pb (48.7 ng·m⁻³) and Ni (2.2 ng·m⁻³) were within the limits set by the WHO (500 ng·m⁻³ for Pb and 25 ng·m⁻³ for Ni). Compared with other cities worldwide (Table S5), the concentrations of Zn, Pb, Cu, and Cr in PM_{2.5} in Beijing throughout the sampling period were lower than those in Taiyuan in the Shanxi province in China [39], Agra in India [40], and Tehran in Iran [41]. The concentrations of As, Cd, and Ni in the province were lower than those in Nanjing [17], Baoding [42], and Gwangju [43], whereas the concentration of Se was higher than that in Taiwan [44].

Compared with the pre-lockdown concentrations, the levels of Zn, Pb, Cd, and Ni decreased by 17.1%, 13.4%, 6.4%, and 20.0% during the full lockdown period in Beijing, respectively, with these elements coming mainly from industrial and motor vehicle emissions [7,26]. Therefore, the results showed that the control measures during the lockdown resulted in lower levels of toxic elements from industrial and traffic emissions. Notably, the concentrations of As, Cu, and Cr increased during the full lockdown period. As is a marker element of coal combustion [14,45]. The presence of Cu and Cr can be attributed to the firework combustion during festivals [46]. Therefore, the unexpected increase in As concentrations may be related to the burning of loose coal for heating in winter, while the unexpected increase in Cu and Cr concentrations may be related to the fireworks set off during the Chinese New Year [47].

3.2. PMF Source Apportionment

3.2.1. Solution Selection and Interpretation

The sample data in this study, collected in Beijing, were used to analyze PMF solutions for three to eight factors. In this study, the Q/Q_{expected} value of each solution was calculated to identify the rational number of factors. Based on the Q/Q_{expected} value for each solution (Figure S3), the Q/Q_{expected} ratio decreased from 1.3 as the resolution factors increased from 4 to 5. On the contrary, a decrease was observed in the Q/Q_{expected} ratio (0.7), indicating an excess fitting of factors from 5 to 6. Therefore, on combining local and regional emissions, the five-factor solutions for Beijing were identified as optimal matches, based on the interpretability of the factors. The resolved factors are dust emissions, coal

combustion, industrial emissions, traffic emissions, and mixed sources of biomass burning and firework combustion.

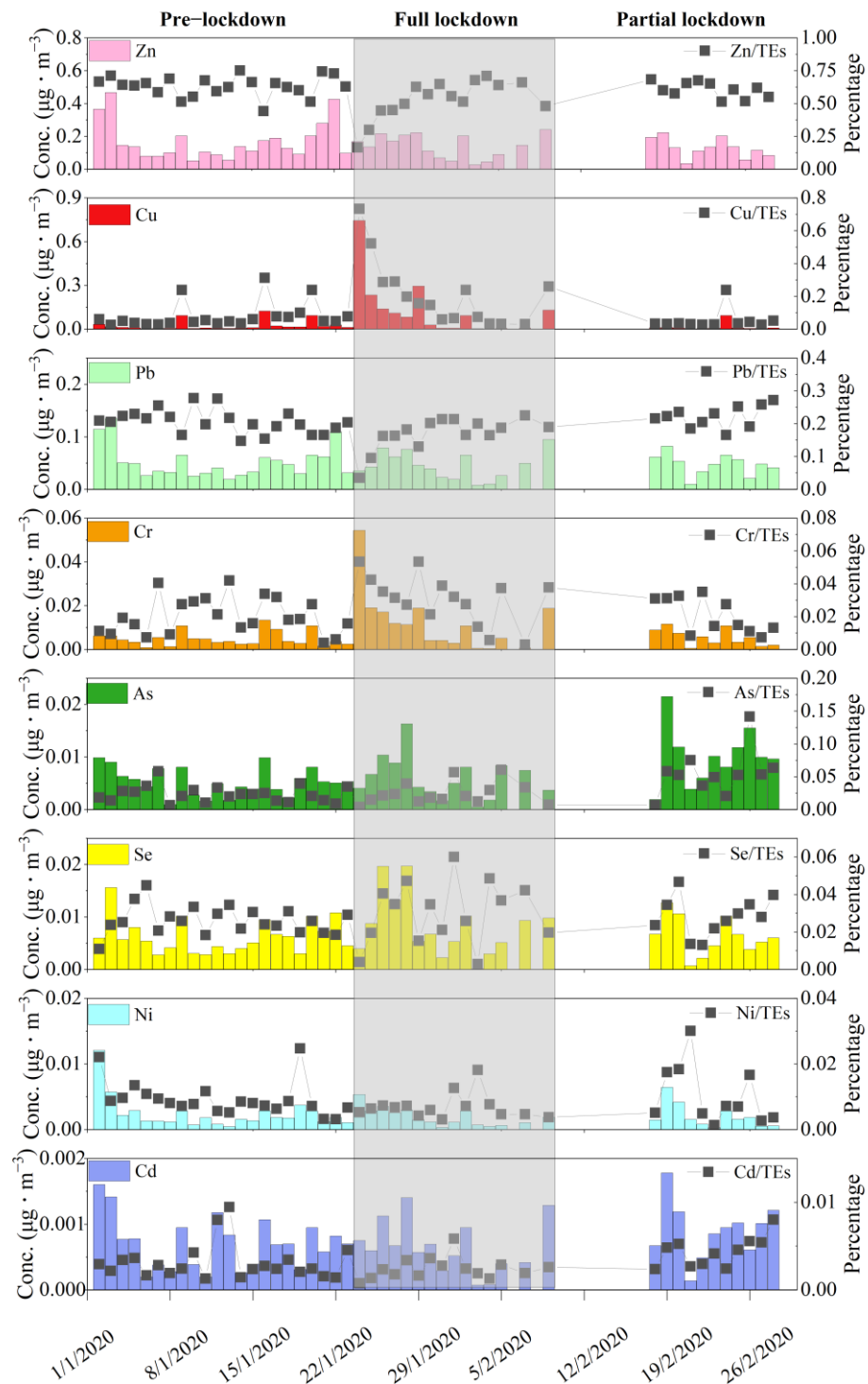


Figure 2. The time series of concentration and percentage of the selected toxic elements (TEs) in Beijing.

The factor profiles for Beijing are presented in Table 2 and Figure 3. Factor 1 (traffic emissions) was characterized by high OC-, EC-, Fe-, Mn-, Zn-, and Pb-related variations. OC and EC derive mainly from vehicular emissions [12,26]. Fe, Mn, and Zn could be discharged from vehicle exhausts and brake wear [8,48]. Tire wear can also produce Zn-containing particles [45], and road paint contains Pb, which is a new emission source [48,49].

Factor 2 (coal combustion) accounted for most variations in OC, EC, Na, As, and Se [6]. According to the emissions inventory, coal combustion in China contributes 74.2% and 64.6% to the total emissions of As and Se, respectively [14]. Factor 3 was characterized by Ca, Na, Mg, and Al. Ca and Mg derive primarily from construction dust and soil dust [14,45]. Al is a typical crustal element [26], and, although Na originates mainly from aged sea salt, it is influenced by road dust. Therefore, Factor 3 represents dust emissions. Factor 4 (V, Cr, Mn, Ni, Se, Cd, and Pb) derives from industrial emissions [7,14]. Cr is applied extensively in industrial production activities, such as electroplating, leather, and metallurgy [50]. Hebei and Shandong provinces are traditional industrial areas that could influence the Beijing–Tianjin–Hebei region through regional transport [14]. Factor 5 (mixed source of biomass burning and fireworks) showed high K, Mg, Al, Cu, and Ba loadings [31,46]. Compounds K, Mg, Al, Cu, and Ba are important materials for manufacturing fireworks, as shown in Supplementary Table S6 [31]. Compounds of K are the main oxidizing agents in fireworks, such as KNO_3 and KClO_3 . Mg and Al are used as the luminous and oxidizing agents, respectively. Ba and Cu compounds are used to produce green and blue flames, respectively. Although Cr originates mainly from industrial production, firework combustion also releases certain amounts of Cr. The Cr compounds are used as oxidizing agents in fireworks and could, therefore, be an important source of Cr during festivals [46]. Additionally, biomass burning, including wood and agricultural residues, emits substantial amounts of K [45]. Accordingly, Factor 5 is a mixed source of biomass burning and firework combustion.

Table 2. Factor profiles resolved via positive matrix factorization (PMF) analysis.

The Factor Profiles	The Main Tracer
Factor 1 (traffic emissions)	OC, EC, Fe, Mn, Zn, and Pb
Factor 2 (coal combustion)	OC, EC, Na, As, and Se
Factor 3 (dust emissions)	Ca, Na, Mg, and Al
Factor 4 (industrial emissions)	V, Cr, Mn, Ni, Se, Cd, and Pb
Factor 5 (mixed source of biomass burning and fireworks)	K, Mg, Al, Cu, and Ba

3.2.2. Source Contributions

The time series of the contributions of different pollution sources in Beijing during the study period are shown in Figure 4. Throughout the study period, the contribution of different pollution sources in Beijing was in the following order: traffic emissions (37.4%) > coal combustion (26.1%) > dust emissions (20.5%) > industrial emissions (9.3%) > mixed source of biomass burning and firework combustion (6.7%). Traffic emissions and coal combustion are important sources of $\text{PM}_{2.5}$ in winter [51,52]. Therefore, Beijing should reinforce control measures on pollution sources related to traffic and coal combustion.

Figure 5 shows the variation of percentage contributions of pollution sources during the different periods in Beijing. During pre-lockdown, traffic emissions were the main pollution sources of $\text{PM}_{2.5}$, accounting for 41.3% of the $\text{PM}_{2.5}$ mass, followed by coal combustion (24.8%) and dust (22.6%). During the full lockdown, the contribution of traffic emissions significantly decreased by 10.9% compared to the emission levels in the pre-lockdown period, while the contributions of coal combustion to toxic elements increased by 5.5%. The contributions of traffic emissions decreased significantly during the full lockdown period as a direct response to the strict measures [22]. Dai et al. [53] also found that coal combustion emissions were dominant during the COVID-19 lockdown. The strict control measures forced people to stay at home, leading to an increase in the energy requirements for heating and cooking. In addition, suburban and rural residential areas consumed more coal during the lockdown [54]. During the full lockdown, the contribution of mixed sources (biomass burning and fireworks) increased significantly by 20.4%, which could be ascribed to the intensive combustion of fireworks during the spring festival, which marks a new year on the lunar calendar. According to Cui et al. [31], the combustion of fireworks contributes 40% of the total element mass in $\text{PM}_{2.5}$ and, therefore, is a significant source of the elements

in PM_{2.5}. In addition, during the period, the contribution of industrial and dust emissions was reduced by 7.1% and 8.0%, respectively. During the partial lockdown period, the contributions of traffic and industrial emissions increased by 8.6% and 8.5% in Beijing, respectively. Traffic emissions have been the main source of PM_{2.5} pollution in Beijing before and during the partial lockdown. Furthermore, during the partial lockdown, the contribution of dust emissions was elevated by 10.0%. In contrast, the contribution of mixed sources (biomass burning and fireworks) and coal combustion decreased by 19.5% and 7.6%, respectively. These results showed that coal combustion, biomass burning, and combustion of fireworks were closely related to people’s heating activities and holiday celebrations.

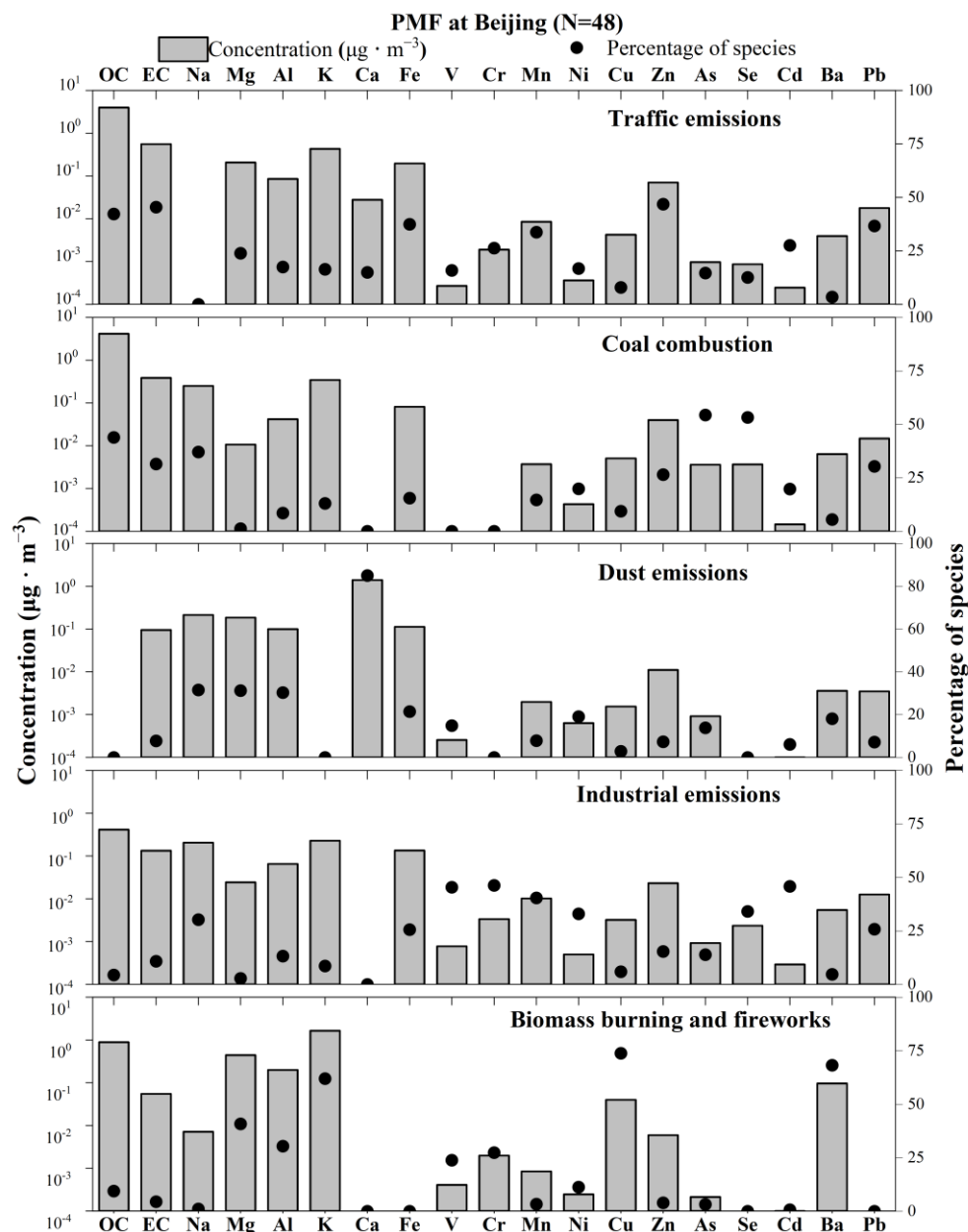


Figure 3. Factor profiles resolved via positive matrix factorization (PMF) analysis (concentration and percentage of species).

3.3. Health Risk Assessment

3.3.1. Non-Carcinogenic Risk in Different Periods

Table S7 and Figure 6a show the non-carcinogenic risks (HIs) via the inhalation route for children and adults in Beijing. According to Equation (1), the magnitude of the HI

was the same for both children and adults. The HI value for selected toxic elements in Beijing during the study period was 0.27, well below the US EPA limit (1.00). The HI here was lower than those in Baoding [52], Linfen [6], and Beijing [8]. This indicated that the HIs of the selected toxic elements during the study period were insignificant for both children and adults. Zhang et al. [33] also determined that the integrated effects of multi-metal exposure might not pose non-carcinogenic risks. Although As was the major contributor to HI, it was below the safety threshold. These results suggest that there was no single-factor non-carcinogenic risk in Beijing. The HIs for both children and adults were below the US EPA limits during different time periods. Compared with the pre-lockdown levels, the HIs for toxic elements in Beijing increased by 14% during the full lockdown period. The highest HQ was for Cu, which increased by 348%. The HQ of Cr (VI) also increased by 146%. Intensive combustion of fireworks during the annual spring festival significantly affects Cu and Cr concentrations [31], and higher Cu and Cr concentrations lead to increased non-carcinogenic risks. The HQs of Zn, Pb, Ni, and Cd showed a decreasing trend, with reductions of 17%, 13%, 20%, and 6%, respectively. The HIs of toxic elements in Beijing increased by 54% during the partial lockdown period, with the most significant increase occurring in the HQs of As and Cd (66% and 38%, respectively), exceeding the pre-lockdown levels 1.9 times and 1.3 times, respectively. Overall, the non-carcinogenic risks of selected toxic elements for children and adults reached the highest levels in Beijing during the partial lockdown but were well below the US EPA limits.

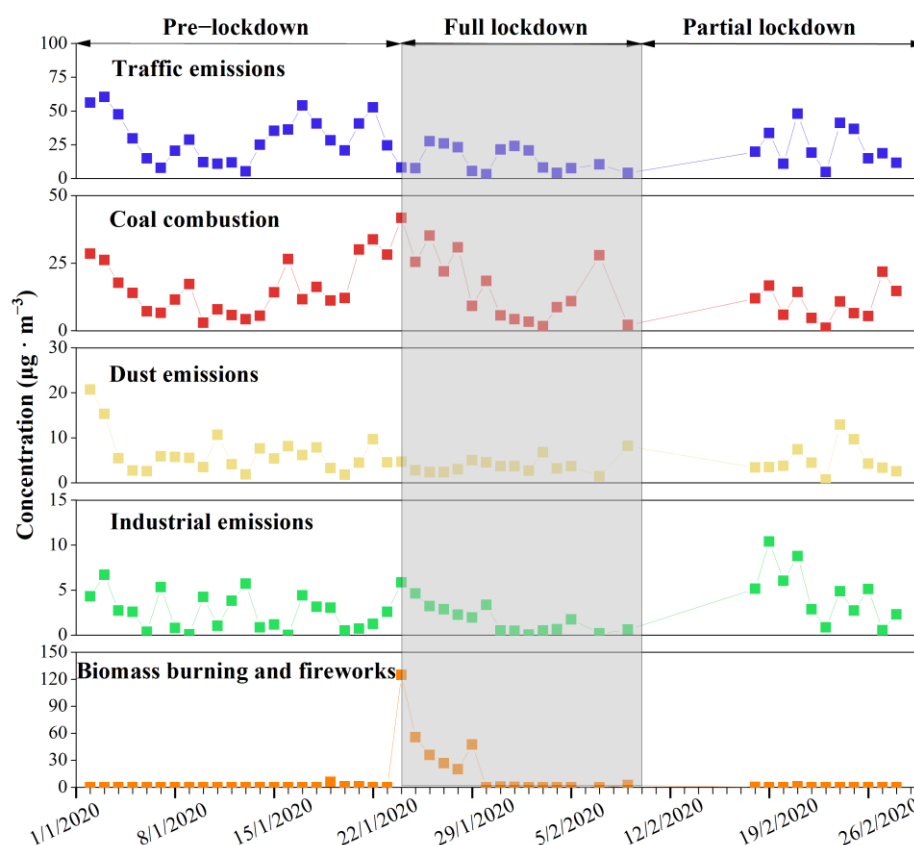


Figure 4. The time series of source contributions to ambient $\text{PM}_{2.5}$ during the sampling period.

3.3.2. Carcinogenic Risk in Different Periods

Table S7 and Figure 6b show the total carcinogenic risk (TCR) via the inhalation route for children and adults in Beijing. The TCRs of the selected toxic elements during the study period for children and adults were 4.98×10^{-6} and 1.99×10^{-5} , respectively. These levels were markedly above the 1.00×10^{-6} limit set by the US EPA which was consistent with the findings of previous risk assessments in major Chinese cities [15], Chennai in India [55],

and Iasi in Romania [56]. Throughout the study period, the TCR was 4.0 times higher in adults than in children, which suggested that adults were a high-cancer-risk group. Adults have a significantly higher risk of cancer [14,30] because the duration of potential exposure is significantly longer for adults than for children [57]. At all time periods, the TCRs for both children and adults exceeded the US EPA standardized limits, and these results indicate a significant carcinogenic risk for both children and adults in Beijing. The CR of Cr (VI) was the highest among the selected toxic elements followed by As at different time periods, indicating that Cr (VI) and As were the key elements constituting cancer risks. This finding is consistent with those for major Chinese cities [10,14,15,44] and Kitakyushu in Japan [33]. Therefore, emission sources related to As and Cr, such as coal combustion, element metallurgy, tanneries, and the combustion of fireworks should be prioritized for appropriate control measures. Compared with their pre-lockdown levels, the TCRs for both children and adults during full lockdown increased by 105%; the CRs of Cr (VI) and As markedly increased by 146% and 14%, while the CRs of Cd, Pb, and Ni decreased by 6%, 13%, and 20%, respectively. During the partial lockdown, the TCRs of the selected toxic elements for both children and adults decreased by 36%, and the CRs of Cr (VI) markedly decreased by 55%, while that of Cd, Pb, As, and Ni increased. Overall, the TCRs of selected toxic elements for children and adults reached the highest levels in Beijing during the full lockdown and were well above the US EPA limits.

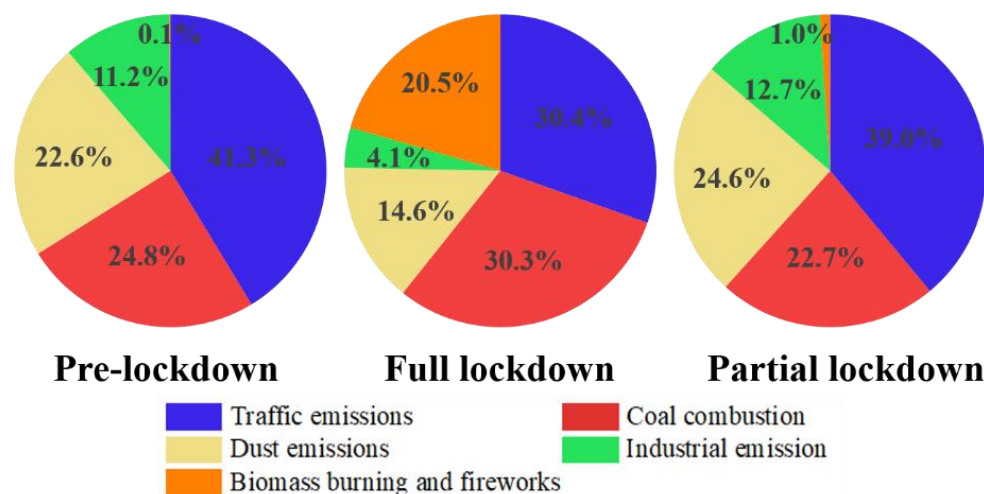


Figure 5. The percentages of source contributions to ambient PM_{2.5} during different COVID-19 lockdown periods.

3.4. Source-Specific Health Risks

3.4.1. Non-Carcinogenic Risks from Different Sources

The non-carcinogenic risks (HIs) of toxic elements (TEs) released from different pollution sources in Beijing are shown in Table S8 and Figure 7a. During the study period, the HI for TEs emitted from coal combustion was 6.84×10^{-2} , which was the greatest contributor to the HIs of the TEs emitted from all sources (43%) and was well below the US EPA standard limits of 1.00. During the pre-lockdown period, coal combustion was the main source of non-carcinogenic risk in Beijing (44%), followed by traffic emissions (21%). During the full lockdown period, coal combustion remained the major source of the total non-carcinogenic risk in Beijing (49%), followed by dust emissions (18%). Compared with the levels for the pre-lockdown period, the HIs from coal combustion, dust emissions, and mixed sources were all significantly increased, with coal combustion and mixed sources (biomass burning and fireworks) contributing the highest elevations in HIs, both increasing by 5%. The higher HI values observed in Beijing during the full lockdown period were ascribed primarily to emissions from these sources. Fan et al. [8] and Yang et al. [14] obtained comparable results. In contrast, the HIs for both traffic and industrial emissions decreased significantly, with their contributions reduced by 8% and

3%, respectively. During partial lockdown, the HI from industrial emissions rose the fastest and even exceeded pre-lockdown levels, and its contribution was elevated by 15%. In addition to industrial emissions, the contribution of traffic emissions to HI was elevated by 7%. Therefore, industrial and traffic emissions contributed the most to the increase in non-carcinogenic risk during partial lockdown. Nevertheless, the HI from coal combustion, dust emissions, and mixed sources (biomass burning and fireworks) considerably declined during the partial lockdown, thereby reducing their contributions to the non-carcinogenic risk by 13%, 4%, and 5%, respectively.

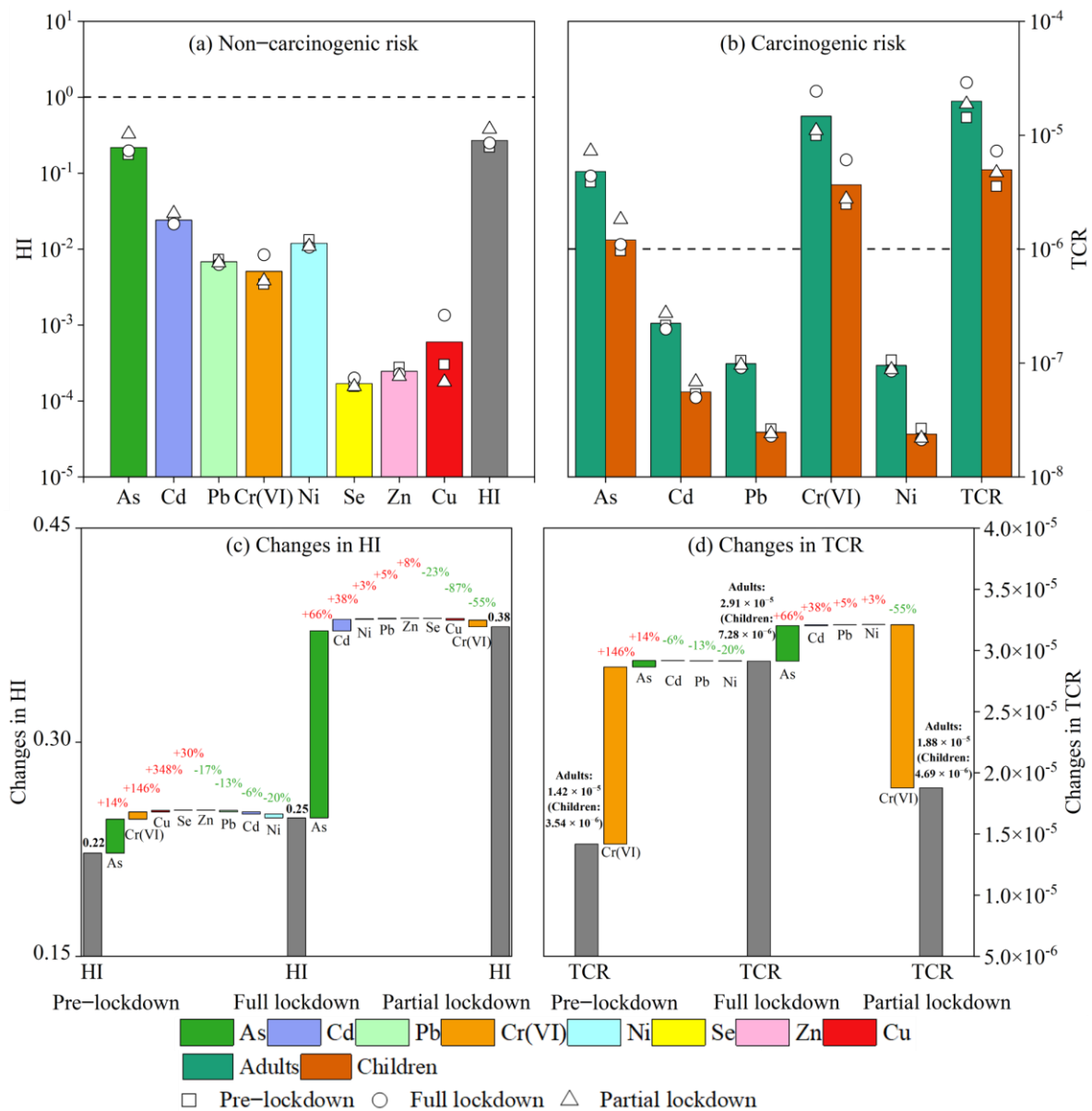


Figure 6. The HI and TCR of the selected TE during the study period and different lockdown periods (the adult non-carcinogenic risk was consistent with that of children; “+ / -” represents an increase or decrease, respectively). (a) non-carcinogenic risk; (b) carcinogenic risk; (c) changes in HI; and (d) changes in TCR.

3.4.2. Carcinogenic Risk from Different Sources

The total carcinogenic risks (TCRs) of toxic elements (TEs) released from different pollution sources in Beijing are shown in Tables S9 and S10 and Figure 7b. The TCRs of the TE industrially emitted for both children and adults (1.55×10^{-6} and 6.19×10^{-6} , respec-

tively) were higher than those of other sources during the study period and significantly exceeded the US EPA limit of 1.00×10^{-6} . Industrial emissions were a major contributor to carcinogenic risk [22,58]. In our study, industrial emissions contributed the most to the pre-lockdown TCR (44%), followed by dust emissions (24%) and coal combustion (19%). Nevertheless, during the full lockdown, the TCRs of all the sources, apart from traffic and industrial emissions, increased significantly, with mixed sources (biomass burning and fireworks) contributing the largest increase in TCRs during full lockdown (26%). Therefore, the control measures aimed at biomass burning and fireworks combustion were essential for the effective reduction in cancer risk. During the partial lockdown, the TCR of industrial emissions rose the fastest, with their contribution to carcinogenic risk increasing by 31% in Beijing. Besides industrial emissions, the contribution of traffic emissions to carcinogenic risk increased by 3%. However, the TCRs from coal combustion, dust emissions, and mixed sources (biomass burning and fireworks) decreased significantly during the partial lockdown, decreasing their contribution to carcinogenic risk by 4%, 3%, and 27%, respectively.

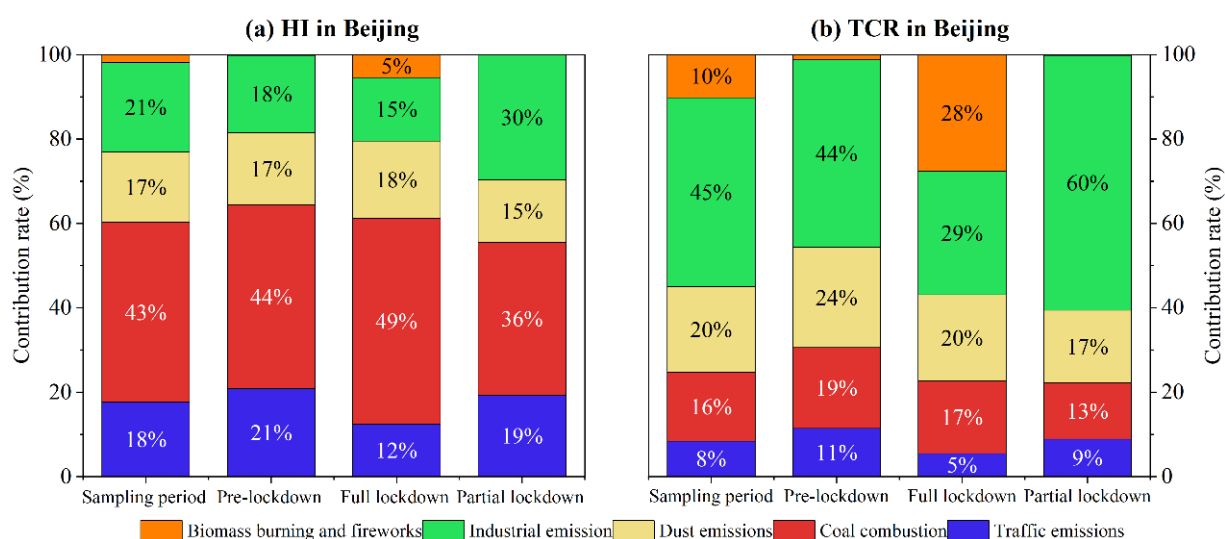


Figure 7. The contribution percentages of HI and TCR of the selected TE sources to the HI and TCR of the TE sources emitted from all emission sources (the contribution percentages for children and adults were the same in this study).

4. Conclusions

The levels of eight toxic elements (Se, Cd, Pb, Zn, As, Cu, Ni, and Cr) in ambient $PM_{2.5}$ were measured in Beijing during the COVID-19 pandemic. The average $PM_{2.5}$ concentration in Beijing during the period of study was $75.1 \mu\text{g}\cdot\text{m}^{-3}$, with the total concentration of the selected toxic elements (TEs) accounting for 0.36% of the $PM_{2.5}$ mass. The most abundant toxic element was Zn ($150.2 \text{ ng}\cdot\text{m}^{-3}$), followed by Pb ($48.7 \text{ ng}\cdot\text{m}^{-3}$). Among the selected TEs, the concentrations of Zn, Pb, Cd, and Ni reduced during the full lockdown. However, unexpected elevations in Se, As, Cu, and Cr concentrations were observed during the full lockdown, which may be related to residential heating activities during the quarantine period as well as firework combustion during the festive season.

Combined with the positive matrix factorization (PMF) model to determine the main pollution sources of $PM_{2.5}$ -bound elements in Beijing. A total of five sources was identified: traffic emission, coal combustion, dust emission, industrial sources and mixed source of biomass burning and firework combustion. Traffic emissions have been the main pollution source in Beijing before, during and in partial lockdown. During the COVID-19 lockdown, the contribution of coal combustion and mixed sources (biomass burning and firework combustion) grew. The contributions of dust, traffic, and industrial emissions rebounded strongly during the partial lockdown, leading to a decline in the contributions of coal combustion and mixed sources (biomass burning and firework combustion).

The health risk (HR) assessment showed the total carcinogenic risks (TCRs) for both children and adults exceeded the threshold (1.00×10^{-6}), with Cr (VI) and As ranking as the two most important elements contributing to TCRs. The TCR for adults was 4 times higher than for children, owing to the duration of potential exposure being longer for adults. In terms of source allocation, coal combustion (43%) is the largest contributor to non-carcinogenic risk (HI) in Beijing, and industrial emissions (45%) are the main contributor to TCRs in children and adults. In addition, the increased contributions of coal combustion and mixed sources (biomass burning and fireworks) were the main contributors to the unexpected elevation of non-carcinogenic and carcinogenic risks in Beijing during full lockdown.

This study combined health risk and source apportionment to provide a multidimensional solution for air pollution control, i.e., from the perspective of source contribution to the mass loads of PM_{2.5}-bound elements, restrictions on traffic emissions should be increased. In addition, from the health risk point of view, priority should be given to the control of pollution sources related to industrial emissions and coal combustion. In the future, Beijing should consider reducing biomass burning and firework combustion to minimize the health impacts of toxic elements such as Cr.

Supplementary Materials: The following are available online at <https://www.mdpi.com/article/10.3390/atmos15050563/s1>, Figure S1: Map of the sampling site in Beijing. Figure S2: Time series of wind speed (WS), temperature and relative humidity (RH) during sampling period in Beijing. Figure S3: The Q/Q_{expected} values and relative contribution of emission sources to PM_{2.5}-bound element mass resolved by PMF model under the different factor numbers. Table S1: Detailed descriptions of the sampling sites. Table S2: Parameters summary for calculating average daily dose. Table S3: The RfC_j and IUR of inhaled health risks for eight selected toxic elements. Table S4: The method detection limits (MDLs) of chemical species resolved in PMF analysis. Table S5: The concentrations of selected toxic elements in PM_{2.5} at different cities worldwide. Table S6: The materials used for producing fireworks. Table S7: The non-carcinogenic (HQ) and carcinogenic risks (CR) in adults and children during the whole sampling period. (The adult non-carcinogenic risk was consistent with that of children). Table S8: The non-carcinogenic risk of toxic elements from emission sources for children and adults during the sampling period and different COVID-19 lockdown periods in Beijing (the adult non-carcinogenic risk was consistent with that of children). (BB & FB: biomass burning and fireworks; DE: dust emissions; CC: coal combustion; IE: industrial emissions; TE: traffic emissions). Table S9: The carcinogenic risk of toxic elements from emission sources for children during the sampling period and different COVID-19 lockdown periods in Beijing. (BB & FB: biomass burning and fireworks; DE: dust emissions; CC: coal combustion; IE: industrial emissions; TE: traffic emissions). Table S10: The carcinogenic risk of toxic elements from emission sources for adults during the sampling period and different COVID-19 lockdown periods in Beijing. (BB & FB: biomass burning and fireworks; DE: dust emissions; CC: coal combustion; IE: industrial emissions; TE: traffic emissions).

Author Contributions: Methodology, M.Z.; Validation, L.R.; Investigation, M.Z., Y.G., G.L. and Y.L.; Writing—original draft, M.Z.; Writing—review & editing, L.R. and X.Y.; Supervision, L.R.; Funding acquisition, L.R. and X.Y. All authors have read and agreed to the published version of the manuscript.

Funding: This research was funded by the National Natural Science Foundation of China, grant number 41705136 and the Special Project for Basic Scientific Research Operations of Central-level Public Welfare Research Institutes, grant number 2019YSKY-025.

Informed Consent Statement: Not applicable.

Data Availability Statement: The data presented in this study are available on request from the corresponding author due to data privacy requirements.

Acknowledgments: Thanks to all the authors for their efforts, especially thanks to the editors and reviewers!

Conflicts of Interest: The authors declare no conflict of interest.

References

1. Bell, M.L.; Ebisu, K.; Leaderer, B.P.; Gent, J.F.; Lee, H.J.; Koutrakis, P. Associations of PM_{2.5} Constituents and Sources with Hospital Admissions: Analysis of Four Counties in Connecticut and Massachusetts (USA) for Persons \geq 65 Years of Age. *Environ. Health Perspect.* **2014**, *122*, 138–144. [[CrossRef](#)]
2. Yao, X.; Gao, M.; Wei, Z.; Chen, M.; Shangguan, W. Removal of hexanal in cooking fume by combination of storage and plasma-catalytic oxidation on alkali-modified Co-Mn solid solution. *Chemosphere* **2019**, *220*, 738–747. [[CrossRef](#)]
3. Deng, Y.; Liu, Y.; Wang, T.; Cheng, H.; Feng, Y.; Yang, Y.; Zhang, L. Photochemical reaction of CO₂ on atmospheric mineral dusts. *Atmos. Environ.* **2020**, *223*, 117222. [[CrossRef](#)]
4. Zheng, J.; Li, M.; Tang, B.; Luo, W.; Mai, B. Levels, Spatial Distribution, and Impact Factors of Heavy Metals in the Hair of Metropolitan Residents in China and Human Health Implications. *Environ. Sci. Technol.* **2021**, *55*, 10578–10588. [[CrossRef](#)]
5. Coleman, N.C.; Burnett, R.T.; Ezzati, M.; Marshall, J.D.; Pope, C.A. Fine Particulate Matter Exposure and Cancer Incidence: Analysis of SEER Cancer Registry Data from 1992–2016. *Environ. Health Perspect.* **2020**, *128*, 107004. [[CrossRef](#)]
6. Wang, Y.; Liu, B.; Zhang, Y.; Dai, Q.; Song, C.; Duan, L.; Guo, L.; Zhao, J.; Xue, Z.; Bi, X.; et al. Potential health risks of inhaled toxic elements and risk sources during different COVID-19 lockdown stages in Linfen, China. *Environ. Pollut.* **2021**, *284*, 117454. [[CrossRef](#)]
7. Yan, R.H.; Peng, X.; Lin, W.; He, L.Y.; Wei, F.H.; Tang, M.X.; Huang, X.F. Trends and Challenges Regarding the Source-Specific Health Risk of PM_{2.5}-Bound Metals in a Chinese Megacity from 2014 to 2020. *Environ. Sci. Technol.* **2022**, *56*, 6996–7005. [[CrossRef](#)]
8. Fan, M.Y.; Zhang, Y.L.; Lin, Y.C.; Cao, F.; Fu, P. Specific sources of health risks induced by metallic elements in PM_{2.5} during the wintertime in Beijing, China. *Atmos. Environ.* **2020**, *246*, 118112.1–118112.11. [[CrossRef](#)]
9. Wu, L.; Luo, X.S.; Li, H.; Cang, L.; Yang, J.; Yang, J.; Zhao, Z.; Tang, M. Seasonal levels, sources, and health risks of heavy metals in atmospheric PM_{2.5} from four functional areas of Nanjing city, eastern China. *Atmosphere* **2019**, *10*, 419. [[CrossRef](#)]
10. Huang, R.-J.; Cheng, R.; Jing, M.; Yang, L.; Li, Y.; Chen, Q.; Chen, Y.; Yan, J.; Lin, C.; Wu, Y.; et al. Source-Specific Health Risk Analysis on Particulate Trace Elements: Coal Combustion and Traffic Emission As Major Contributors in Wintertime Beijing. *Environ. Sci. Technol.* **2018**, *52*, 10967–10974. [[CrossRef](#)] [[PubMed](#)]
11. Jahan, Z.; Khan, L.; Sun, Y.; Tian, G.; Shi, Y.; Feng, Y. Chemical characterization and source apportionment of PM₁ and PM_{2.5} in Tianjin, China: Impacts of biomass burning and primary biogenic sources. *J. Environ. Sci.* **2021**, *99*, 196–209.
12. Zhang, W.; Peng, X.; Bi, X.; Cheng, Y.; Feng, Y. Source apportionment of PM_{2.5} using online and offline measurements of chemical components in Tianjin, China. *Atmos. Environ.* **2021**, *244*, 117942. [[CrossRef](#)]
13. Hua, W.; Wu, B. Atmospheric circulation anomaly over mid- and high-latitudes and its association with severe persistent haze events in Beijing. *Atmos. Res.* **2022**, *277*, 106315. [[CrossRef](#)]
14. Yang, X.; Zheng, M.; Liu, Y.; Yan, C.; Liu, J.; Liu, J.; Cheng, Y. Exploring sources and health risks of metals in Beijing PM_{2.5}: Insights from long-term online measurements. *Sci. Total Environ.* **2021**, *814*, 151954. [[CrossRef](#)]
15. Li, F.; Yan, J.; Wei, Y.; Zeng, J.; Lü, G. PM_{2.5}-bound heavy metals from the major cities in China: Spatiotemporal distribution, fuzzy exposure assessment and health risk management. *J. Clean. Prod.* **2020**, *286*, 124967. [[CrossRef](#)]
16. Betha, R.; Behera, S.N.; Balasubramanian, R. 2013 Southeast Asian smoke haze: Fractionation of particulate-bound elements and associated health risk. *Environ. Sci. Technol.* **2014**, *48*, 4327–4335. [[CrossRef](#)] [[PubMed](#)]
17. Li, H.; Wang, Q.G.; Shao, M.; Wang, J.; Wang, C.; Sun, Y.; Qian, X.; Wu, H.; Yang, M.; Li, F. Fractionation of airborne particulate-bound elements in haze-fog episode and associated health risks in a megacity of southeast China. *Environ. Pollut.* **2016**, *208*, 655–662. [[CrossRef](#)]
18. Tan, J.; Zhang, L.; Zhou, X.; Duan, J.; Li, Y.; Hu, J.; He, K. Chemical characteristics and source apportionment of PM_{2.5} in Lanzhou, China. *Sci. Total Environ.* **2017**, *601–602*, 1743–1752. [[CrossRef](#)]
19. Hsu, C.Y.; Chi, K.H.; Wu, C.D.; Lin, S.L.; Chen, Y.C. Integrated analysis of source-specific risks for PM_{2.5}-bound metals in urban, suburban, rural, and industrial areas. *Environ. Pollut.* **2021**, *275*, 116652.1–116652.8. [[CrossRef](#)] [[PubMed](#)]
20. Liu, J.; Chen, Y.; Chao, S.; Cao, H.; Zhang, A.; Yang, Y. Emission control priority of PM_{2.5}-bound heavy metals in different seasons: A comprehensive analysis from health risk perspective. *Sci. Total Environ.* **2018**, *644*, 20–30. [[CrossRef](#)]
21. Xu, X.; Hu, X.; Wang, T.; Sun, M.; Wang, L.; Zhang, L. Non-inverted U-shaped challenges to regional sustainability: The health risk of soil heavy metals in coastal China. *J. Clean. Prod.* **2020**, *279*, 123746. [[CrossRef](#)]
22. Wang, H.; Miao, Q.; Shen, L.; Yang, Q.; Wu, Y.; Wei, H. Air pollutant variations in Suzhou during the 2019 novel coronavirus (COVID-19) lockdown of 2020: High time-resolution measurements of aerosol chemical compositions and source apportionment. *Environ. Pollut.* **2020**, *271*, 116298. [[CrossRef](#)]
23. Liu, S.; Wu, T.; Wang, Q.; Zhang, Y.; Tian, J.; Ran, W.; Cao, J. High time-resolution source apportionment and health risk assessment for PM_{2.5}-bound elements at an industrial city in northwest China. *Sci. Total Environ.* **2023**, *870*, 161907. [[CrossRef](#)]
24. Lin, Y.C.; Zhang, Y.L.; Song, W.; Yang, X.; Fan, M.Y. Specific sources of health risks caused by size-resolved PM-bound metals in a typical coal-burning city of northern China plain during the winter haze event. *Sci. Total Environ.* **2020**, *734*, 138651. [[CrossRef](#)]
25. Xie, J.; Jin, L.; Cui, J.; Luo, X.S.; Li, X.D. Health risk-oriented source apportionment of PM_{2.5}-associated trace metals. *Environ. Pollut.* **2020**, *262*, 114655. [[CrossRef](#)]
26. Diao, L.; Zhang, H.; Liu, B.; Dai, C.; Feng, Y. Health risks of inhaled selected toxic elements during the haze episodes in Shijiazhuang, China: Insight into critical risk sources. *Environ. Pollut.* **2021**, *276*, 116664.1–116664.12. [[CrossRef](#)]

27. Huang, C.; Wang, Y.; Li, X.; Ren, L.; Cao, B. Clinical features of patients infected with 2019 novel coronavirus in Wuhan, China. *Lancet* **2020**, *395*, 497–506. [[CrossRef](#)]
28. Tu, W.; Tang, H.; Chen, F.; Wei, Y.; Xu, T.; Liao, K.; Xiang, N.; Shi, G.; Li, Q.; Feng, Z. Epidemic Update and Risk Assessment of 2019 Novel Coronavirus—China, January 28, 2020. *China CDC Wkly.* **2020**, *2*, 83–86. [[CrossRef](#)]
29. Dai, Q.; Liu, B.; Bi, X.; Wu, J.; Liang, D.; Zhang, Y.; Feng, Y.; Hopke, P.K. Dispersion Normalized PMF Provides Insights into the Significant Changes in Source Contributions to PM_{2.5} after the COVID-19 Outbreak. *Environ. Sci. Technol.* **2020**, *54*, 9917–9927. [[CrossRef](#)]
30. Wang, G.; Huang, K.; Fu, Q.; Chen, J.; Huo, J.; Zhao, Q.; Duan, Y.; Lin, Y.; Yang, F.; Zhang, W.; et al. Response of PM_{2.5}-bound elemental species to emission variations and associated health risk assessment during the COVID-19 pandemic in a coastal megacity. *J. Environ. Sci.* **2022**, *122*, 115–127. [[CrossRef](#)]
31. Cui, Y.; Ji, D.; Maenhaut, W.; Gao, W.; Zhang, R.; Wang, Y. Levels and sources of hourly PM_{2.5}-related elements during the control period of the COVID-19 pandemic at a rural site between Beijing and Tianjin. *Sci. Total Environ.* **2020**, *744*, 140840. [[CrossRef](#)] [[PubMed](#)]
32. IARC. *IARC Monographs on the Identification of Carcinogenic Hazardous to Humans*; International Agency for Research on Cancer, World Health Organization: Lyon, France, 2021.
33. Zhang, X.; Eto, Y.; Aikawa, M. Risk assessment and management of PM_{2.5}-bound heavy metals in the urban area of Kitakyushu, Japan. *Sci. Total Environ.* **2021**, *795*, 148748. [[CrossRef](#)] [[PubMed](#)]
34. US EPA. *Risk Assessment Guidance for Superfund Volume I: Human Health Evaluation Manual (Part F: Supplemental Guidance for Inhalation Risk Assessment)*; EPA-540-R-070-002; Office of Superfund Remediation and Technology Innovation, U.S. Environmental Protection Agency: Washington, DC, USA, 2009.
35. Hopke, P.K.; Dai, Q.; Li, L.; Feng, Y. Global review of recent source apportionments for airborne particulate matter. *Sci. Total Environ.* **2020**, *740*, 140091. [[CrossRef](#)] [[PubMed](#)]
36. Paatero, P.; Tapper, U. Positive matrix factorization: A non-negative factor model with optimal utilization of error estimates of data values. *Environmetrics* **1994**, *5*, 111–126. [[CrossRef](#)]
37. Zhang, J.; Zhou, X.; Wang, Z.; Yang, L.; Wang, J.; Wang, W. Trace elements in PM_{2.5} in Shandong Province: Source identification and health risk assessment. *Sci. Total Environ.* **2018**, *621*, 558–577. [[CrossRef](#)] [[PubMed](#)]
38. Ma, T.; Duan, F.; Ma, Y.; Zhang, Q.; Xu, Y.; Li, W.; Zhu, L.; He, K. Unbalanced emission reductions and adverse meteorological conditions facilitate the formation of secondary pollutants during the COVID-19 lockdown in Beijing. *Sci. Total Environ.* **2022**, *838*, 155970. [[CrossRef](#)] [[PubMed](#)]
39. Liu, K.; Ren, J. Characteristics, sources and health risks of PM_{2.5}-bound potentially toxic elements in the northern rural China. *Atmos. Pollut. Res.* **2019**, *10*, 1621–1626. [[CrossRef](#)]
40. Agarwal, A.; Mangal, A.; Satsangi, A.; Lakhani, A.; Kumari, K.M. Characterization, sources and health risk analysis of PM_{2.5} bound metals during foggy and non-foggy days in sub-urban atmosphere of Agra. *Atmos. Res.* **2017**, *197*, 121–131. [[CrossRef](#)]
41. Mohsenibandpi, A.; Eslami, A.; Ghaderpoori, M.; Shahsavani, A.; Alinejad, A. Health risk assessment of heavy metals on PM_{2.5} in Tehran air, Iran. *Data Brief* **2018**, *17*, 347–355. [[CrossRef](#)]
42. Liang, B.; Li, X.L.; Ma, K.; Liang, S.X. Pollution characteristics of metal pollutants in PM_{2.5} and comparison of risk on human health in heating and non-heating seasons in Baoding, China. *Ecotoxicol. Environ. Saf.* **2018**, *170*, 166–171. [[CrossRef](#)]
43. Park, S.S.; Jung, S.A.; Gong, B.J.; Cho, S.Y.; Lee, S.J. Characteristics of PM_{2.5} Haze Episodes Revealed by Highly Time-Resolved Measurements at an Air Pollution Monitoring Supersite in Korea. *Aerosol. Air Qual. Res.* **2013**, *13*, 957–976. [[CrossRef](#)]
44. Tsai, P.-J.; Young, L.-H.; Hwang, B.-F.; Lin, M.-Y.; Chen, Y.-C.; Hsu, H.-T. Source and health risk apportionment for PM_{2.5} collected in Sha-Lu area, Taiwan. *Atmos. Pollut. Res.* **2020**, *11*, 851–858. [[CrossRef](#)]
45. Park, J.; Kim, H.; Kim, Y.; Heo, J.; Kim, S.-W.; Jeon, K.; Yi, S.M.; Hopke, P.K. Source apportionment of PM_{2.5} in Seoul, South Korea and Beijing, China using dispersion normalized PMF. *Sci. Total Environ.* **2022**, *833*, 155056. [[CrossRef](#)]
46. Kong, S.; Li, L.; Li, X.; Yin, Y.; Chen, K.; Liu, D.; Yuan, L.; Zhang, Y.J.; Shan, Y.P.; Ji, Y.Q. The impacts of firework burning at the Chinese Spring Festival on air quality: Insights of tracers, source evolution and aging processes. *Atmos. Chem. Phys.* **2015**, *15*, 2167–2184. [[CrossRef](#)]
47. Cheng, K.; Chang, Y.; Kuang, Y.; Khan, R.; Zou, Z. Elucidating the responses of highly time-resolved PM_{2.5} related elements to extreme emission reductions. *Environ. Res.* **2022**, *206*, 112624. [[CrossRef](#)]
48. Wang, J.M.; Jeong, C.H.; Hilker, N.; Healy, R.M.; Sofowote, U.; Deboasz, J.; Su, Y.; Munoz, A.; Evans, G.J. Quantifying metal emissions from vehicular traffic using real world emission factors. *Environ. Pollut.* **2020**, *268*, 115805. [[CrossRef](#)]
49. O’Shea, M.J.; Krekeler, M.P.S.; Vann, D.R.; Gieré, R. Investigation of Pb-contaminated soil and road dust in a polluted area of Philadelphia. *Environ. Monit. Assess.* **2021**, *193*, 440. [[CrossRef](#)]
50. Li, X.; Jiang, L.; Bai, Y.; Yang, Y.; Liu, S.; Chen, X.; Xu, J.; Liu, Y.; Wang, Y.; Guo, X.; et al. Wintertime aerosol chemistry in Beijing during haze period: Significant contribution from secondary formation and biomass burning emission. *Atmos. Res.* **2019**, *218*, 25–33. [[CrossRef](#)]
51. Grange, S.K.; Fischer, A.; Zellweger, C.; Alastuey, A.; Querol, X.; Jaffrezo, J.-L.; Weber, S.; Uzu, G.; Hueglin, C. Switzerland’s PM₁₀ and PM_{2.5} environmental increments show the importance of non-exhaust emissions. *Atmos. Environ.* **2021**, *12*, 100145. [[CrossRef](#)]

52. Shen, Y.-W.; Zhao, H.; Zhao, C.-X.; Dong, S.-F.; He, K.-Q.; Xie, J.-J.; Lv, M.L.; Yuan, C.G. Temporal responses of PM_{2.5}-bound trace elements and health risks to air control policy in a typical northern city in China during 2016–2020. *J. Clean. Prod.* **2023**, *408*, 137165. [[CrossRef](#)]
53. Dai, Q.; Ding, J.; Hou, L.; Li, L.; Cai, Z.; Liu, B.; Song, C.; Bi, X.; Wu, J.; Zhang, Y.; et al. Haze episodes before and during the COVID-19 shutdown in Tianjin, China: Contribution of fireworks and residential burning. *Environ. Pollut.* **2021**, *286*, 117252.1–117252.7. [[CrossRef](#)] [[PubMed](#)]
54. Shen, H.; Shen, G.; Chen, Y.; Russell, A.G.; Hu, Y.; Duan, X.; Meng, W.; Xu, Y.; Yun, X.; Lyu, B.; et al. Increased air pollution exposure among the Chinese population during the national quarantine in 2020. *Nat. Hum. Behav.* **2021**, *5*, 239–246. [[CrossRef](#)] [[PubMed](#)]
55. Peter, A.E.; Nagendra, S.M.S.; Nambi, I.M. Comprehensive analysis of inhalable toxic particulate emissions from an old municipal solid waste dumpsite and neighborhood health risks. *Atmos. Pollut. Res.* **2018**, *9*, 1021–1031. [[CrossRef](#)]
56. Galon-Negru, A.G.; Olariu, R.I.; Arsene, C. Size-resolved measurements of PM_{2.5} water-soluble elements in Iasi, north-eastern Romania: Seasonality, source apportionment and potential implications for human health. *Sci. Total Environ.* **2019**, *695*, 133839. [[CrossRef](#)]
57. US EPA. *Risk Assessment Guidance for Superfund Volume I: Human Health Evaluation Manual (Supplemental Guidance)*; OSWER Directive: 9285.6-03; Office of Emergency and Remedial Response, U.S. Environmental Protection Agency: Washington, DC, USA, 1991.
58. Duan, X.; Yan, Y.; Li, R.; Deng, M.; Peng, L. Seasonal variations, source apportionment, and health risk assessment of trace metals in PM_{2.5} in the typical industrial city of Changzhi, China. *Atmos. Pollut. Res.* **2020**, *12*, 365–374. [[CrossRef](#)]

Disclaimer/Publisher’s Note: The statements, opinions and data contained in all publications are solely those of the individual author(s) and contributor(s) and not of MDPI and/or the editor(s). MDPI and/or the editor(s) disclaim responsibility for any injury to people or property resulting from any ideas, methods, instructions or products referred to in the content.